



Ultimate Resistance of Reinforced Concrete Columns Strengthened with Angles and Battens: Theoretical Model and Experimental Validation

Rosario Montuori¹, Vincenzo Piluso², Gianvittorio Rizzano³

SUMMARY

In this paper, the results of an experimental program dealing with the evaluation of the behaviour of R/C columns confined by means of angles and battens are presented. The tests have been planned after the calibration of an analytical model for predicting the load carrying capacity of strengthened and unstrengthened columns which is able to account for many parameters often neglected in the current design practice. Starting from the experimental results, the proposed model has been improved. Finally, the load carrying capacity of tested specimens has been evaluated also according to the provisions of Eurocode 8 in order to analyse its accuracy.

INTRODUCTION

Even though the strengthening of reinforced concrete columns with angles and battens has been described in a lot of engineering manuals since several decades ago, the problem is often treated in a qualitative way rather than in a quantitative one, with only rough indications devoted to the evaluation of the load carrying capacity of the strengthened member.

With reference to the problem of seismic retrofitting of existing buildings, it is evident that the need to provide designers with a valid calculation methodology which accounts for many parameters often neglected in current design practice.

The methodology used in this work, already presented by the authors [1, 2], accounts for the following issues which are relevant to an accurate evaluation of the ultimate resistance of the strengthened column: the deformations resulting from the loads acting on the original pre-existing section; the effect of the different behavior of effectively confined concrete with respect to the unconfined one; the variation of effectively confined concrete area as a consequence of the strengthening intervention; the variation of the σ - ϵ law for the effectively confined concrete due to the increase of “confining” steel (the battens); the possibility of buckling of longitudinal bars. In addition, depending on the kind of structural detail adopted at the beam-to-column joint location, the angles can be considered as acting both in tension and in compression, only in tension or, finally, they can be considered as providing a confining effect only. The results of an experimental program which has been carried out at the laboratory of Civil Engineering

¹ PhD in Structural Engineering - Department of Civil Engineering – University of Salerno

² Full Professor in Structural Engineering - Department of Civil Engineering – University of Salerno

³ Researcher in Structural Engineering - Department of Civil Engineering – University of Salerno

Department of Salerno University are herein presented to validate of the proposed methodology and to grasp the possible revisions to improve the calculation model. Furthermore, a comparison with the recommendations provided by Eurocode 8 is also carried out.

THEORETICAL MODEL

The proposed theoretical model is based on a stress-strain constitutive law which can be defined of “last generation”. This law is different for different zones of the same section depending on the fact that they can be considered effectively confined or not by the actions of the lateral reinforcement, both existing hoops and additional battens. Therefore, in the same section two different constitutive laws have been adopted: one for the effectively confined concrete and another one for the unconfined concrete (Figure 1).

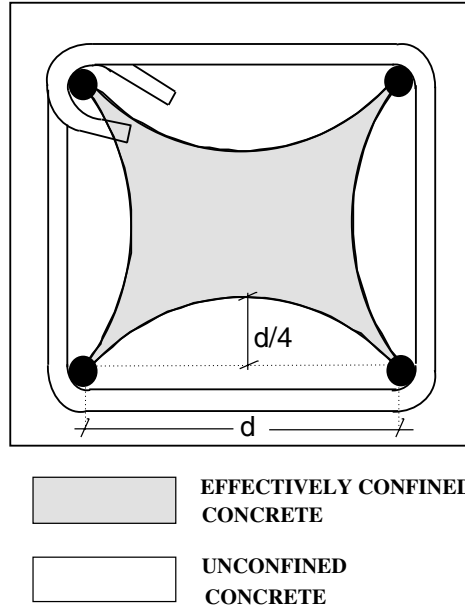


Figure 1: concrete confinement

The concrete model

The adopted concrete model, which has been recently proposed by Mander et al. [3, 4], is very different, both in terms of strength and of ductility, for effectively confined concrete and for unconfined concrete. It is based on the following relationship:

$$\sigma_c = \frac{f_{cc} \chi^r}{r - 1 + \chi^r} \quad (1)$$

with:

$$f_{cc} = f_c \left(2.254 \sqrt{1 + \frac{7.94 f_l}{f_c}} - 2 \frac{f_l}{f_c} - 1.254 \right) \quad (2)$$

$$\varepsilon_{cc} = 0.002 \left[1 + 5 \left(\frac{f_{cc}}{f_c} - 1 \right) \right] \quad (3)$$

$$\chi = \frac{\varepsilon_c}{\varepsilon_{cc}} \quad (4)$$

$$r = \frac{E_c}{E_c - E_{sec}} \quad (5)$$

$$E_{sec} = \frac{f_{cc}}{\epsilon_{cc}} \quad (6)$$

$$E_c = 5000\sqrt{f_c} \quad (MPa) \quad (7)$$

where f_c is the cylindrical compression strength of the unconfined concrete and ϵ_c is the corresponding strain; f_{cc} is the cylindrical compression strength of the confined concrete and ϵ_{cc} is the corresponding strain; E_{sec} and E_c (Figure 2) represent, respectively, the secant and tangent elastic modulus; f_y is the yield stress of the confining steel (hoops); s and A_s are, respectively, the spacing and the area of the hoops. Finally, f_l represents the lateral confining stress, which for a circular section having diameter D and cover concrete c is equal to:

$$f_l = 0.95 \frac{2f_y A_s}{(D - 2c)s} \quad (8)$$

It is interesting to note that in case of confining stress equal to zero, relationships (2) and (3) provide, respectively, $f_{cc} = f_c$ and $\epsilon_{cc} = \epsilon_{co} = 0.002$, i.e. the maximum stress and the corresponding strain of the unconfined concrete. The whole representation of the constitutive law for the unconfined concrete is obtained using relationship (1) up to a deformation equal to a $2\epsilon_{co}$ is achieved. Starting from this strain, the tangent to the obtained curve has to be calculated and the point ϵ_{sp} corresponding to the ultimate strain of the unconfined concrete can be computed maintaining the same gradient (Figure 2).

In the case of rectangular sections, the evaluation of f_{cc} can be performed by means of the abacus depicted in Figure 3.

For the use of this abacus it is necessary to determine the confining stresses f_{l1} e f_{l2} provided by:

$$f_{l1} = \min(f_{lx}, f_{ly}) \quad f_{l2} = \max(f_{lx}, f_{ly}) \quad (9)$$

with:

$$f_{lx} = 0.75f_y\rho_x \quad f_{ly} = 0.75f_y\rho_y \quad (10)$$

being:

$$\rho_x = \frac{n_{bx}A_s(b-2c)}{s(b-2c)(h-2c)} \quad \text{and} \quad \rho_y = \frac{n_{by}A_s(h-2c)}{s(b-2c)(h-2c)} \quad (11)$$

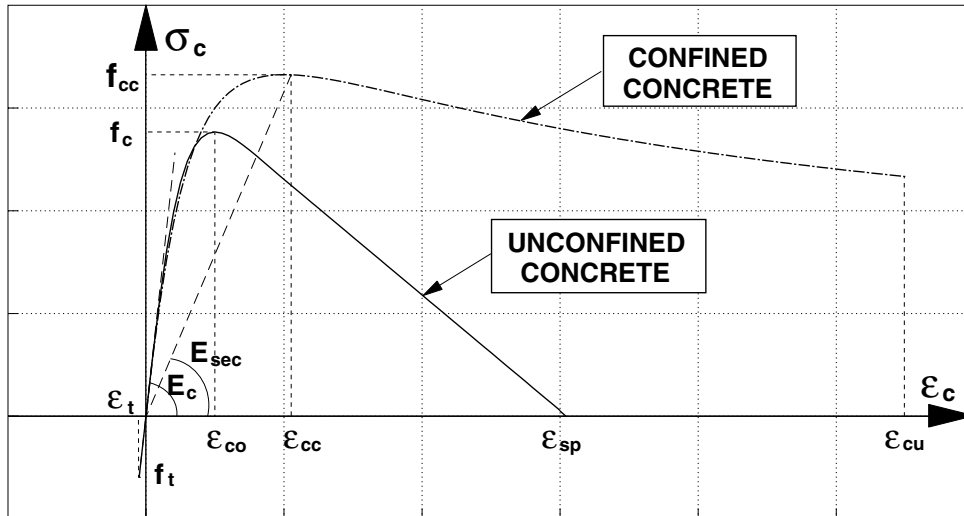


Figure 2: σ - ϵ constitutive law for concrete modelling

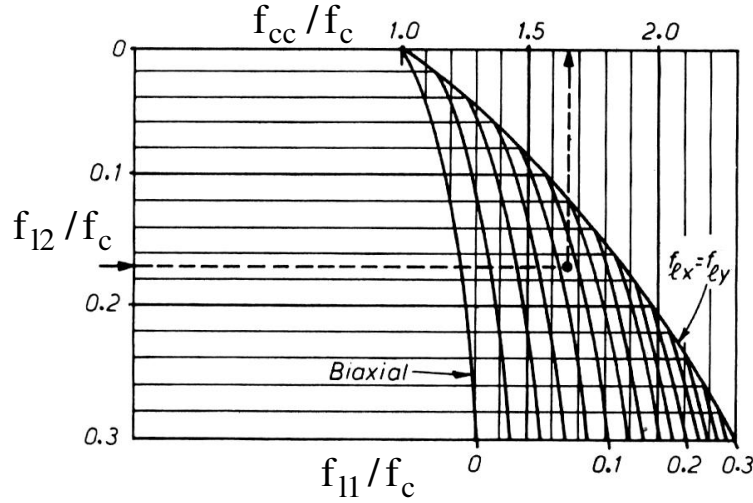


Figure 3: abacus for the evaluation of f_{cc} for rectangular sections

where b , h and c represent, respectively, the base, the height and the cover concrete of the section, n_{bx} and n_{by} represent the sum of the number of hoop arms and the number of additional ties in the direction parallel to b and h , respectively. In addition, aiming to a complete description of the constitutive law it is necessary to determine the ultimate strain ε_{cu} which can be estimated by means of the following relationship:

$$\varepsilon_{cu} = 0.004 + \frac{1.4 f_y \rho_s \varepsilon_{su}}{f_{cc}} \quad (12)$$

where ε_{su} represents the ultimate steel strain and ρ_s is the volumetric ratio of confining steel which is equal to $\rho_x + \rho_y$ for rectangular sections and to $4A_s / [(D-2c)s]$ for circular sections. Finally, the tension strength is equal to f_t , both for confined and unconfined concrete, taken as:

$$f_t = 0.5 \sqrt{f_c} \quad (\text{MPa}) \quad (13)$$

The modulus of elasticity in tension is equal to the one in compression.

The steel model

The assumed modeling for the steel behavior is depicted in Figure 4, where ε_{sy} is the yield stress, ε_{sh} is the strain corresponding to the beginning of strain hardening, determined as $\varepsilon_{sh} = 10\varepsilon_{sy}$, and ε_{su} is the ultimate strain, determined as $\varepsilon_{su} = 100\varepsilon_{sy}$. The hardening can be represented by means of a second order curve expressed as:

$$\sigma_s = f_y \left[\frac{f_u}{f_y} - \left(\frac{f_u}{f_y} - 1 \right) \left(\frac{\varepsilon_{su} - \varepsilon_s}{\varepsilon_{sh} - \varepsilon_{su}} \right)^2 \right] \quad (14)$$

where f_u is the ultimate strength.

The constitutive law, above described, can be used only for bars in tension. In fact, if the bar is compressed and the concrete constituting the cover has been spalled, the possibility of buckling has to be considered. Obviously, in this way it is assumed that unconfined concrete represents a lateral rigid restraint for the longitudinal bars and it is able to avoid the buckling up to the achievement of its ultimate deformation. This assumption provides the minimum effect in terms of resistance degradation due to buckling. In fact, if the unconfined concrete is, conversely, assumed to be unable to laterally restrain the bars before the achievement of its ultimate deformation, the bars can be prematurely subjected to buckling and themselves give rise to the spalling of the cover concrete.

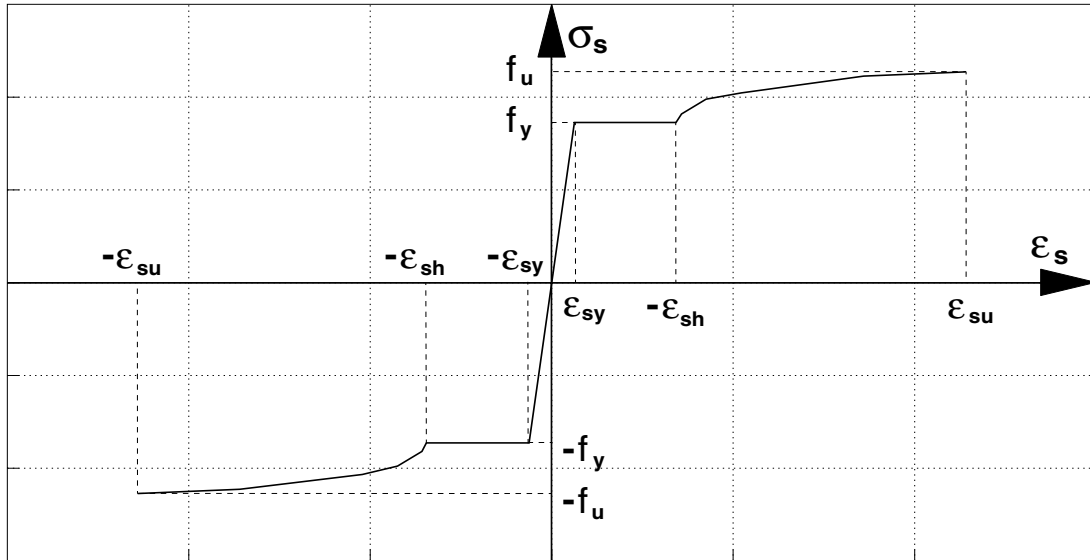


Figure 4: σ - ϵ constitutive law for steel

In Figure 5 a possible kinematic mechanism for a buckled longitudinal bar is depicted. The hoops can be considered as simple support restraints, so that the bar is modelled as a continuous beam on simple supports subjected to a compression axial load. Obviously, increasing the axial load, the part of the bar between two consecutive hoops can develop a kinematic mechanism characterized by three plastic hinges (Figure 5). The equilibrium of the part of the bar located between two consecutive hoops provides:

$$N = \frac{2M_p}{w} \quad (15)$$

where M_p is the yielding moment of the bar cross section and w is the lateral displacement. In addition, the longitudinal displacement δ and the rigid rotation θ are related by means of the following relationship:

$$\delta = s - 2(s/2) \cos \theta = s(1 - \cos \theta) \quad (16)$$

where s represents the spacing of the hoops.

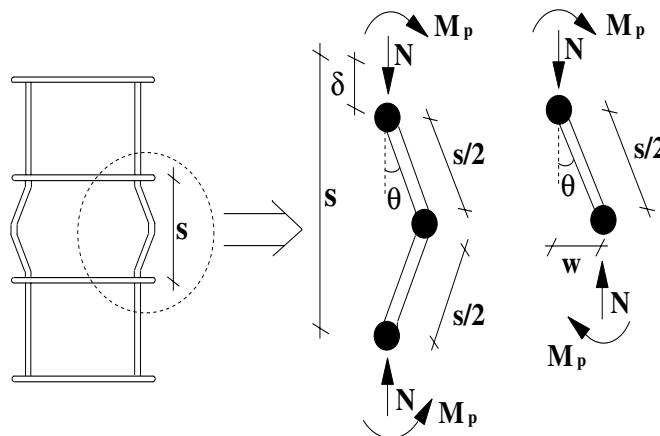


Figure 5: kinematic mechanism of a buckled bar

Deriving $\cos\theta$ from equation (16), the longitudinal displacement w can be expressed as:

$$w = \frac{s}{2} \text{sen}\theta = \frac{s}{2} \sqrt{1 - \cos^2\theta} = \frac{s}{2} \sqrt{2 \frac{\delta}{s} - \frac{\delta^2}{s^2}} \quad (17)$$

By substituting the above expression of w into equation (15), the relation $N - \delta$ between the axial load and the longitudinal displacement, i.e. between the average stress $\sigma_s = N/A_l$ (with A_l = cross section area of the longitudinal bar) and the axial deformation $\varepsilon_s = \delta/s$ of the buckled bar is obtained:

$$\sigma_s = \frac{4M_p}{sA_l \sqrt{2\varepsilon - \varepsilon^2}} \quad (18)$$

The above relation, when M_p is considered as constant, does not take into account the interaction between the axial load and the bending moment, i.e. the reduction of plastic bending moment of the bar due to the axial load in the bar. Aiming to account for the described effect, it is necessary to use the relation existing between N and $M_p(N)$ based on the plastic distribution of stresses depicted in Figure 6. With reference to such figure, it results:

$$N = R^2 (\pi - 2\phi + \text{sen}2\phi) f_y \quad (19)$$

$$M_p(N) = \frac{4}{3} R^3 f_y \text{sen}^3 \phi \quad (20)$$

where f_y is the steel yield stress, R is the radius of the bar cross section and ϕ identifies the neutral axis of the cross section.

The use of relationships (18), (19), and (20) leads to an iterative procedure. In fact, for a fixed value of the axial deformation ε , and for a starting value of the neutral axis given by $\phi = \pi/2$, equation (18) provides the value of the average stress in the bar and the corresponding axial load $N = \sigma_s A_l$ which can be introduced in equation (19) aiming to the correction of the neutral axis position given by ϕ . The obtained ϕ value allows, by means of equation (20), the calculation of the reduced yielding moment which has to be used in equation (18) to correct the value of the average stress of the bar. The procedure continues until convergence is reached.

To complete the $\sigma - \varepsilon$ curve of the bar, it is necessary to define the point from which relation (18) has to be used. In fact, considering the critical load equal to the Eulerian one, the curve is completely determined as shown in Figure 7. In the same figure it is also represented the influence of the reduction of the yielding moment due to the axial load.

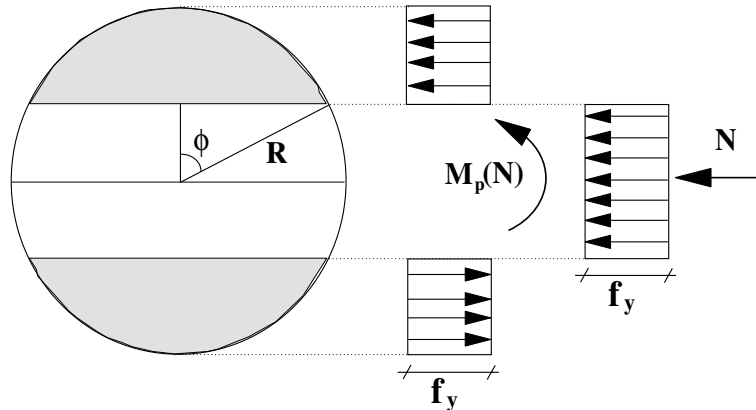


Figure 6: Tension plastic distribution

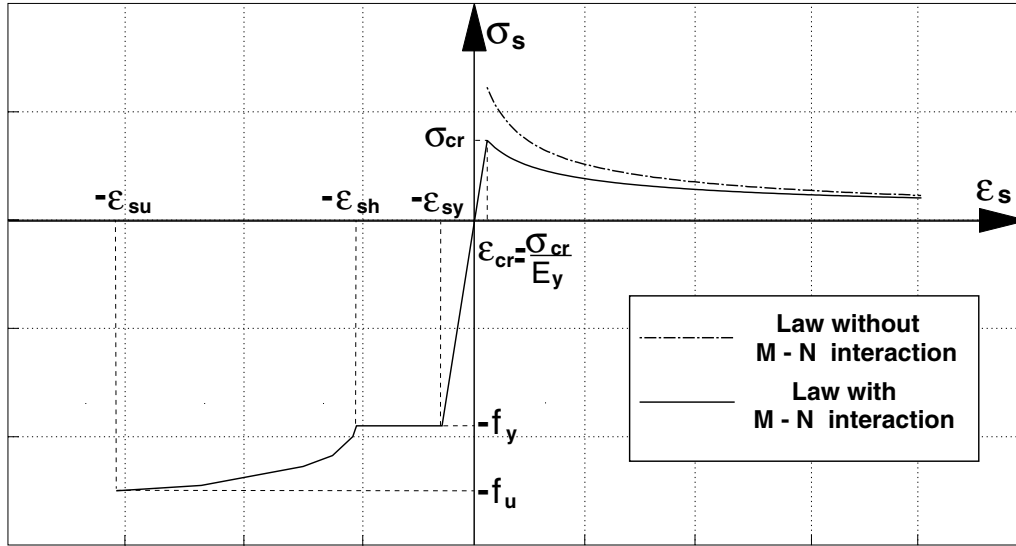


Figure 7: σ - ϵ law for a bar with buckling in compression

The moment-curvature diagram

Starting from the σ - ϵ models previously described, with reference to a reinforced concrete section, a procedure for computing the moment-curvature diagram can be easily outlined.

The cross section has been subdivided into elementary square elements which have been characterized by an appropriate constitutive law: confined concrete, unconfined concrete, steel of the longitudinal reinforcement or steel of the strengthening angles. If the effect of the load acting on the unstrengthened element has to be considered, then the deformations existing in each element before the strengthening intervention have to be computed and considered in the subsequent analysis.

The different zones of the section, effectively confined and unconfined, need to be preliminarily detected. To this aim, the longitudinal “confining bars” or “restraining bars”, which are those located in the corners or those out of corners, but restrained by steel ties, have to be identified. Starting from these restraining points, it is possible to determine the arches of parabola dividing the zones of effectively confined concrete from the zones of unconfined concrete [7], as it is shown in Figure 1 for the unstrengthened original existing section and in Figure 8 for the strengthened section.

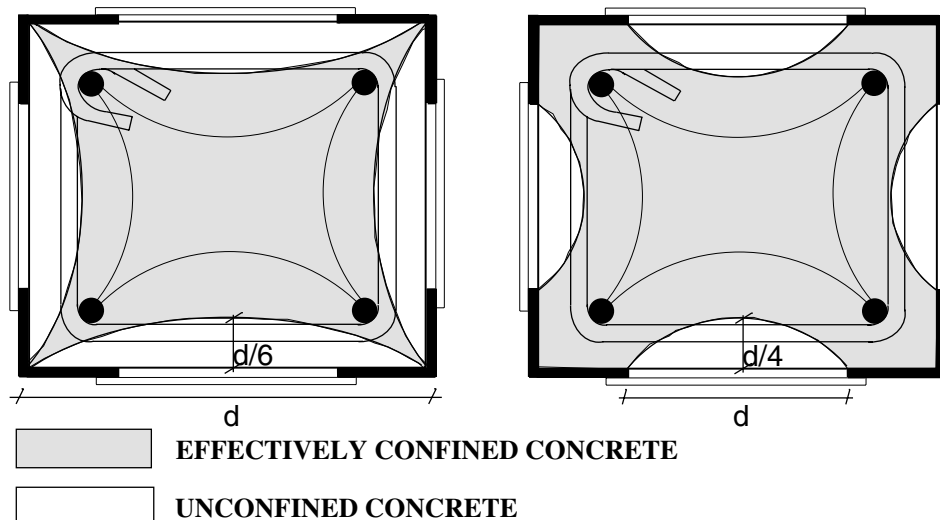


Figure 8: different models for identifying confined and unconfined concrete

It is important to analyze the possible confining action due to the angles. In Figure 8, two different degree of confinement due to the angles are shown. The first one is represented by the case in which the confining action is exerted along the entire leg of the angles and the second one in which the confining action is located at the point corresponding to the angle corner. The first model has been adopted by the authors in previous works [1, 2] while the second model has been suggested by the results of the experimental tests discussed in the following sections. In addition, the confining effect due to the angles will be considered, in the following analyses, considering two values (4 and 6) for the span-to-depth ratio of the parabola separating confined and unconfined concrete.

On the bases of the constitutive laws of steel, confined concrete and unconfined concrete, the procedure for evaluating the moment-curvature diagram, for a given axial load has been codified into computer program namely SCAB (Strengthened Columns with Angles and Battens). In this code, the buckling of longitudinal bars occurs when the cover represented by the unconfined concrete is completely collapsed. This condition is reached when the concrete deformation is equal to the ultimate one [5]. Therefore, it is assumed that the unconfined concrete, before its ultimate deformation is achieved, is able to laterally restrain the longitudinal bars preventing their premature instability. It is necessary to underline that, this assumption can lead to an underestimation of the effects of buckling of longitudinal bars which can precede the attainment of the ultimate deformation of the unconfined concrete with the spalling of the cover concrete.

THE EXPERIMENTAL TESTS

The experimental tests have been performed on 13 prismatic specimens characterised by a square section with a side length equal to 15 cm and height equal to about 50 cm. The longitudinal bar diameter is equal to 10 and 16 mm while the diameter of the stirrups and of the transversal connecting bars is equal to 6 mm. 8 specimens have been reinforced with angles (30x30x2 mm) and battens (15x3 mm). The specimens have been subjected to eccentric axial load under axial displacement control. In Table 1 and Table 2, the values of all the geometrical properties of tested specimens are given with reference to the symbols depicted in Figure 9. The values of the cross-section dimension of the specimens reinforced with angles include the thickness of the angles which is equal to 6 mm.

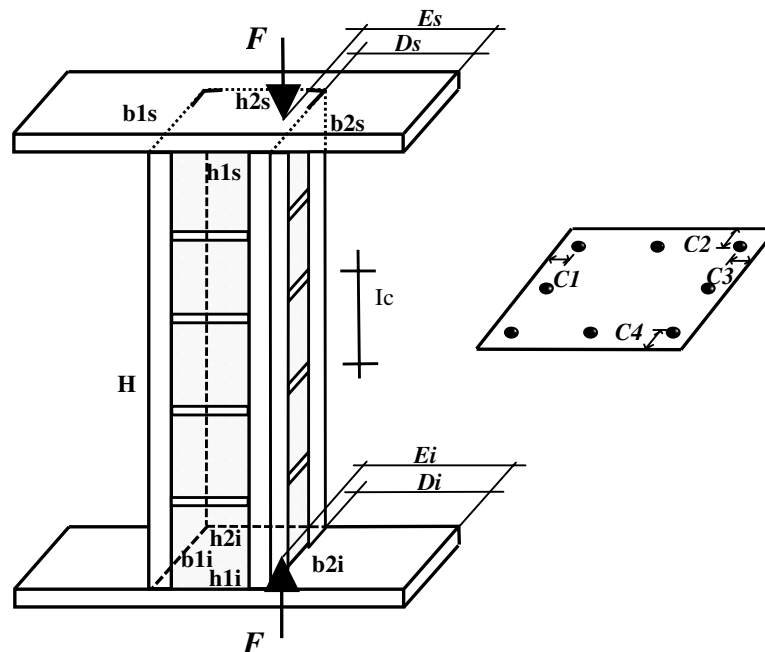


Figure 9: geometry of tested specimens

Table 1: adopted eccentricity, longitudinal bars and type of structural detail

Unstrengthened specimens	
$8\phi 10$ with $e=h/2$	A-NR
$8\phi 10$ with $e=h/3$	B-NR
$8\phi 10$ with ties and $e=h/2$	C-NR
$4\phi 16$ with $e=h/2$	D-NR
$4\phi 16$ with $e=h/3$	E-NR
Strengthened specimens	
$8\phi 10$ with $e=h/2$	A-R1
$8\phi 10$ with $e=h/3$	B-R1a
$8\phi 10$ with $e=h/3$	B-R1b
$8\phi 10$ with ties and $e=h/2$	C-R1
$4\phi 16$ with $e=h/2$	D-R1
$4\phi 16$ with $e=h/2$ with angles acting only in compression	D-R2
$4\phi 16$ with $e=h/2$ with angles not acting both in tension and in compression	D-R3
$4\phi 16$ with $e=h/3$	E-R1

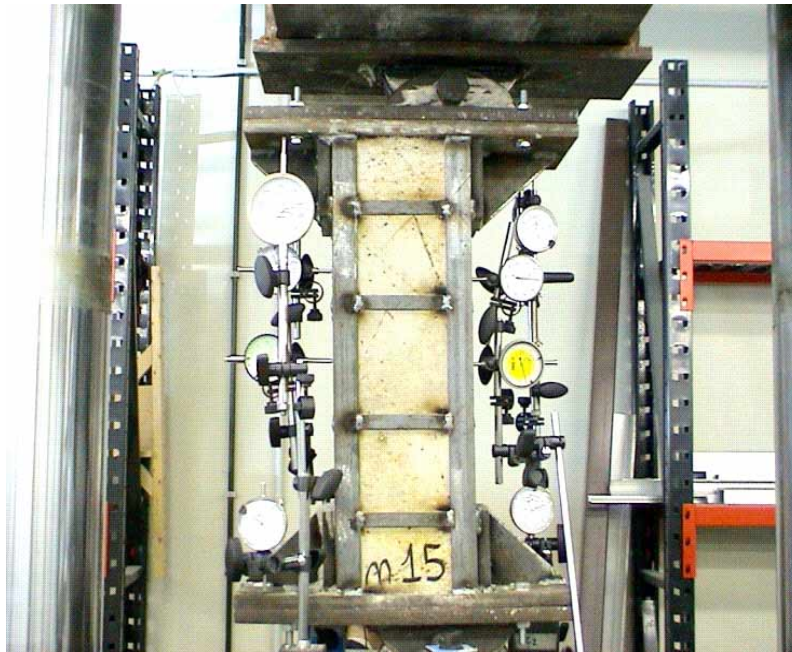


Figure 10: a tested specimen

The experimental tests have been carried out with a constant eccentricity by hinging the specimen ends at the testing machine, Schenck RBS 4000 E2, by means of an appropriate system made of steel plates as shown in Figure 10. Such system has been adopted to apply two different eccentricities. In order to determine the stress-strain law of the materials constituting the specimens, the longitudinal bars, the hoops, the angles and the battens have been subjected to standard coupon tests. In addition, the cubic strength of concrete has been also determined. The average values of both the yield strength and the ultimate strength of steel elements are given in Table 3.

Concerning the concrete strength, five specimens have been obtained from the same mix, the corresponding ultimate stress is provided in Table 4. The scatter is significant (about 23% with respect to the maximum value) and, obviously, affects the degree of refinement of the theoretical model.

Table 2: geometry of tested specimens (cm)

UNSTRENGTHENED SPECIMENS												
Specimen	H1s	H2s	B1s	B2s	H1i	H2i	B1i	B2i	Ds	Es	Di	Ei
A-NR	15.5	15.5	15.3	16	15.3	15.3	15.5	16	12.2	12.7	12	12.7
B-NR	15.5	15.7	15.8	15.7	15.5	15.7	15.8	16	12	15	12	15.6
C-NR	15.4	15.4	15.6	15.8	15.7	15.7	15.6	15.7	12.3	12.5	12.1	12.8
D-NR	15	15.5	14.8	14.8	15	15.5	15	15	13	12.1	13	12.9
E-NR	15.9	15.4	15.8	15.6	16	15.4	15.7	15.6	11.4	12.8	11.7	15.4
	C1	C2	C3	C4								
A-NR	2	2.4	2	2								
B-NR	2.4	1.8	2.5	1.8								
C-NR	2.1	2.1	2.1	2.2								
D-NR	2.2	2.5	2.2	2.1								
E-NR	2.6	2.7	2.7	2.7								
STRENGTHENED SPECIMENS												
Specimen	H1s	H2s	B1s	B2s	H1i	H2i	B1i	B2i	Ds	Es	Di	Ei
A-R1	16.2	16.2	17	16.5	16.2	16.2	17	16.5	11.5	12.3	11.5	12.3
B-R1a	16.3	16.6	16.3	16.7	16.2	16.5	16.6	16.4	11.6	14.7	11.5	15.3
B-R1b	16.1	16.1	16.8	16.7	16	16.2	16.8	16.7	12.2	14.7	12	15.4
C-R1	16.5	15.7	16.8	16.8	16.3	16	17	16.8	11.9	12.3	12.1	12.5
D-R1	16.1	16.7	16.6	16.7	15.8	16.3	16.6	16.5	11.6	12.1	12.5	12.5
D-R2	16.9	17.3	17	17	17	17.6	17.1	16.9	11.1	12.2	11	12.6
D-R3	16.2	16.8	16.7	16.7	16.5	17.2	16.2	16.4	11.5	12.4	11.3	12.8
E-R1	16.5	16.7	16.5	16.7	16.4	17	16.7	16.8	13	14.8	11.6	15.3
		C1	C2	C3	C4	Ic						
A-R1		2	2.4	2	2.4	12						
B-R1a		2.2	2.2	2.4	2.2	11.3						
B-R1b		2.5	2.2	2.5	2.2	11.7						
C-R1		2.2	2	2.3	2	11.2						
D-R1		2.5	2.9	2.8	2.5	11.3						
D-R2		2.5	2.6	3.2	2.3	8.6						
D-R3		2.4	3.1	3.3	2.9	8.3						
E-R1		2.7	2.8	2.8	2.7	11.3						

Table 3: yield and ultimate strength steel of elements

Steel type	f_y (N/mm ²)	f_u (N/mm ²)
Bar ϕ 10	491	593
Bar ϕ 16	539	655
Hoops	350	454
Angles	353	508
Battens	291	465

Table 4: cubic resistance of concrete

Concrete specimen	R_{cub} (N/mm ²)
1	25.5
2	28.1
3	33.0
4	27.0
5	27.2

EUROCODE 8 PROVISIONS

According to Eurocode 8, the confining effect of a steel jacket can be evaluated in the same way as for hoops and ties using for the geometric steel ratio, in each transverse direction, the cross-sectional area of steel relative to a vertical section through the column.

The strength of confined concrete can be evaluated as:

$$f_{cc} = f_{cd} \left[1 + 0.37 \left(\frac{0.5\alpha\rho_s f_{yw}}{f_{cd}} \right) \right]^{0.87} \quad (21)$$

where α is the so-called efficiency factor given by the ratio of the confined concrete area to the total area defined as:

$$\alpha = \left(1 - \frac{s_h}{2b_c} \right) \left(1 - \frac{s_h}{2h_c} \right) \left(1 - \frac{\sum b_i^2}{6h_c b_c} \right) \quad (22)$$

In the above relationships, f_{yw} is the yield strength of the jacketing steel, s_h is the batten spacing, b_c and h_c are the dimensions of the concrete core, b_i represents the distance between restrained (by means of ties or hoops) longitudinal bars along the perimeter and ρ_s is the geometric steel ratio which is not explicitly defined in Eurocode 8. It seems to be reasonable to take such parameter equal to:

$$\rho_s = \frac{2A_{bat}b_c}{b_c h_c s_h} + \frac{2A_{bat}h_c}{b_c h_c s_h} \quad (23)$$

where A_{bat} represents the batten cross-section area.

Regarding the ultimate deformation of concrete, it is given by:

$$\varepsilon_{cu} = 0.004 + 0.6 \frac{\rho_s \varepsilon_{su} f_{yw}}{f_{cc}} \quad (24)$$

Concerning ε_{su} , there is not any explicit value suggested in Eurocode 8. It seems reasonable to refer this value to the real ultimate deformation of the jacketing steel, i.e., similarly to the proposed model, to a value equal to $100 \times \varepsilon_{sy}$.

The constitutive law used for concrete is the parabola-rectangle model with ultimate strength and ultimate deformation obtained, respectively, from equations (21) and (24). Obviously, the comparison between the theoretical model and the experimental tests has been performed considering an f_{cd} value equal to $0.83 \times R_c$, where R_c is cubic ultimate strength obtained from tested concrete specimens. As specified in Eurocode 8, the concrete properties of the jacketed column are considered to apply over the full section of the member.

Concerning the steel, an elastic perfectly plastic model has been adopted, with a yield stress equal to experimental one.

OBTAINED RESULTS

In order to investigate the influence of the variability of concrete resistance, as testified by experimental evidence (Table 4), the theoretical analyses have been carried out considering three different values of the ultimate strength: the minimum, the average and the maximum one. These three values are equal, respectively, to 25.5N/mm², 28.1N/mm² and 33.0N/mm². The results obtained adopting a span-to-depth ratio equal to 4 for the parabola separating confined and unconfined concrete are given in Table 5. Regarding strengthened specimens the four corner of the angles have been considered as “constraining points”, as shown in the left part of Figure 8.

The results provided in

Table 6 differ from those provided in Table 5 due to a different assumption concerning the span-to-depth ratio of the parabola separating confined and unconfined concrete which have been selected equal to 6.

Finally, in Table 7 the results obtained by means of Eurocode 8 provisions are given. Clearly, in this last case the analyses have been carried out only for the strengthened specimens.

In each table, the percentage errors obtained by the application of the theoretical model, herein suggested, with respect to the experimental value are also given.

In addition, with reference to unstrengthened specimens and with reference to strengthened ones having angles acting both in tension and in compression, the average percentage error is also provided (fat values) in Tables 5, 6 and 7.

Regarding the angle and batten design it has to be underlined that the batten spacing has been designed by imposing a sufficiently small value of the angle slenderness to prevent buckling.

Table 5: results obtained with span-to-depth ratio of the parabola separating confined and unconfined concrete equal to 4

Specimen	Ultimate experimental load [kN]	$R_{c,min} = 25.5 \text{ N/mm}^2$		$R_{c,av} = 28.16 \text{ N/mm}^2$		$R_{c,max} = 33.0 \text{ N/mm}^2$		Variation
		Maximum calculated load [kN]	e[%]	Maximum calculated load [kN]	e[%]	Maximum calculated load [kN]	e[%]	
<i>A-NR</i>	341.6	301	-11,88%	315	-7,79%	340	-0,47%	11,41
<i>B-NR</i>	463.9	403	-13,14%	425	-8,39%	465	0,22%	13,36
<i>C-NR</i>	331.1	302	-8,81%	314	-5,19%	336	1,45%	10,26
<i>D-NR</i>	386.8	341	-11,85%	354	-8,49%	379	-2,03%	9,82
<i>E-NR</i>	551.6	499	-9,54%	523	-5,19%	566	2,60%	12,14
			-11,04%		-6,99%		0,35%	
<i>A-R1</i>	523.9	483	-7,81%	498	-4,95%	524	0,01%	7,82
<i>B-R1a</i>	716.8	629	-12,25%	651	-9,18%	688	-4,02%	8,23
<i>B-R1b</i>	675.5	595	-11,92%	614	-9,11%	648	-4,08%	7,84
<i>C-R1</i>	508.4	466	-8,34%	478	-5,98%	500	-1,65%	6,69
<i>D-R1</i>	555.7	518	-6,79%	533	-4,09%	562	1,12%	7,91
<i>E-R1</i>	745.4	657	-11,86%	679	-8,91%	720	-3,41%	8,45
			-9,82%		-7,03%		-2,00%	
<i>D-R2</i>	580.0	545	-6,15%	561	-3,39%	591	1,77%	7,92
<i>D-R3</i>	493.0	407	-17,60%	423	-	451	-8,70%	8,90
					14,36%			

Table 6: results obtained with span-to-depth ratio of the parabola separating confined and unconfined concrete equal to 6

Specimen	Ultimate experimental load [kN]	$R_{c,min} = 25.5 \text{ N/mm}^2$		$R_{c,av} = 28.16 \text{ N/mm}^2$		$R_{c,max} = 33.0 \text{ N/mm}^2$		Variation
		Maximum calculated load [kN]	e[%]	Maximum calculated load [kN]	e[%]	Maximum calculated load [kN]	e[%]	
<i>A-NR</i>	341.6	306	-10,42	319	-6,61	343	0,41	10,83
<i>B-NR</i>	463.9	408	-12,06	429	-7,53	468	0,87	12,93
<i>C-NR</i>	331.1	305	-7,91	317	-4,28	339	2,36	10,27
<i>D-NR</i>	386.8	344	-11,08	358	-7,46	381	-1,52	9,56
<i>E-NR</i>	551.6	502	-9,00	526	-4,65	568	2,96	11,96
			-10,09		-6,11		1,02	
<i>A-R1</i>	523.9	516	-1,51	530	1,16	554	5,74	7,25
<i>B-R1a</i>	716.8	670	-6,53	695	-3,05	735	2,53	9,06
<i>B-R1b</i>	675.5	636	-5,85	656	-2,89	692	2,43	8,28
<i>C-R1</i>	508.4	499	-1,85	511	0,51	531	4,44	6,29
<i>D-R1</i>	555.7	544	-2,11	559	0,58	587	5,62	7,73
<i>E-R1</i>	745.4	694	-6,86	716	-3,94	756	1,42	8,31
			-4,12		-1,27		3,70	
<i>D-R2</i>	580.0	579	-0,29	596	2,63	624	7,45	7,74
<i>D-R3</i>	493.0	446	-9,70	462	-6,46	488	-1,20	8,5

Table 7: result obtained by means of Eurocode 8 provisions

Specimen	Ultimate experimental load [kN]	$R_{c,min} = 25.5 \text{ N/mm}^2$		$R_{c,av} = 28.16 \text{ N/mm}^2$		$R_{c,max} = 33.0 \text{ N/mm}^2$		Variation
		Maximum calculated load [kN]	e[%]	Maximum calculated load [kN]	e[%]	Maximum calculated load [kN]	e[%]	
<i>A-R1</i>	523.9	531	1,35%	553	5,55%	593	13,18%	11,83
<i>B-R1a</i>	716.8	682	-4,86%	713	-0,54%	769	7,27%	12,13
<i>B-R1b</i>	675.5	650	-3,78%	679	0,51%	732	8,36%	12,14
<i>C-R1</i>	508.4	517	1,69%	536	5,42%	569	11,91%	10,22
<i>D-R1</i>	555.7	561	0,95%	584	5,09%	624	12,28%	11,33
<i>E-R1</i>	745.4	711	-4,61%	741	-0,59%	794	6,52%	11,13
			-1,54%		2,57%		9,92%	
<i>D-R2</i>	580.0	629	8,31%	650	11,93%	691	18,99%	10,68
<i>D-R3</i>	493.0	490	0,62%	513	3,86%	552	11,75%	11,13

It could seem strange that specimen DR2 (with angles acting only in compression) has a resistance (580.0kN) greater than the one (555.7kN) of specimen DR1(theoretically the same as DR2 but with angle acting both in tension and in compression). The apparent inconsistency can be immediately explained by noting that the actual measured dimensions of DR2 specimen are greater than the corresponding ones of DR1 specimen (Table 2).

The results obtained by the application of the proposed methodology (Table 5 and Table 6) could suggest the use of a span-to-depth ratio equal to 6 for the parabola separating confined and unconfined concrete, rather than the value 4 commonly suggested in the technical literature. However, as few experimental data are available, this issue deserves further investigations.

Regarding the points which have to be considered as “restraining”, the analyses have pointed out that the assumption corresponding to the left side of Figure 8 leads to the best agreement with experimental results. However, also this issue could be refined, because, obviously, the truth is in the middle. In fact, starting from the corner of the angle, that is certainly a restraining point, the zones of effectively confined concrete extend themselves towards the end of the flange as a function of the flange stiffness. At present, this limit seems to be more close to the corner of the angle rather than to the end of the flange.

As it can be noted, the prediction made on the base of Eurocode 8 are quite satisfactory. However, it has to be underlined that code provisions do not suggest any rule to account for the load acting on the unstrengthened original cross section and one the role of the hoops existing in the unstrengthened original cross section. Conversely, the numerical procedure herein suggested is able to explicitly consider the deformations caused by the load acting on the unstrengthened cross section before the strengthening intervention. This is an important aspect, because it represents the actual situation of retrofitting where a part of the permanent loads is acting on the original unstrengthened section.

CONCLUSIONS

In this work a rational methodology for analyzing reinforced concrete columns strengthened with angles and battens has been presented. The results obtained with such methodology have been compared with a set of experimental tests. The different behaviour of the confined and unconfined concrete, the possibility of buckling of the longitudinal bars, and the influence of the adopted structural details are explicitly considered.

In fact, the first effect induced by the strengthening intervention is represented by the increase of the effectively confined area. A second effect corresponds to the improvement of the degree of confining action on the concrete that was already confined before the strengthening intervention. In fact, the constitutive laws of the confined concrete are characterized by the increase of its resistance and ductility when the amount of the additional reinforcements increases.

In addition, a third factor is represented by the lateral restrain provided by the cover concrete preventing the buckling of the bars which, on the contrary, can arise in the case of unstrengthened sections. The first case occurs for reinforcements located at the section corners when the strengthening is realized by means of steel angles. In fact, due to the presence of the steel angles, the reinforcements located at the section corners are surrounded by very well confined concrete which cannot be spalled, so that it represents an effective lateral restrain preventing the buckling of the bars. This positive effect can be extended to other internal bars in function of the geometrical dimensions.

Finally, the presence of angles can constitute an effective increase of longitudinal reinforcement depending on the adopted structural detail. If the angles can be realized without any interruption due to the horizontal structural elements, or if the structural detail of the joint is able to transfer the stresses from one storey to the following one, they can be considered acting both in tension and in compression.

The obtained results, considering the great variability of the concrete strength, are in a good agreement with the experimental tests. Finally, also the Eurocode 8 provisions seem to be sufficiently accurate.

REFERENCES

1. MONTUORI R., PILUSO V. “Analisi della capacità portante di colonne in cemento armato rinforzate mediante angolari e calastrelli”, XVIII Congresso C.T.A., Venezia, 26-28 Settembre, 2001.
2. MONTUORI R., RIZZANO G., PILUSO V. “Analisi teorico - sperimentale della capacità portante di colonne in c.a. pressoinflesse rinforzate con angolari e calastrelli, V Workshop italiano sulle strutture composte” - Università degli studi di Salerno 28-29 Novembre 2002 (in press).

3. MANDER J. B., PRIESTLEY M. J. N. AND PARK R. "Theoretical Stress-Strain Model for Confined Concrete", Journal of Structural Engineering, ASCE, 1988: Vol. 114, No.8 pp. 1804-1826.
4. MANDER J. B., PRIESTLEY M. J. N. AND PARK R. "Observed Stress-Strain Behavior of Confined Concrete. Journal of Structural Engineering", ASCE, 1988: Vol. 114, No.8 pp. 1827-1849.
5. APPLETON J. AND GOMES A. "Nonlinear cyclic stress-strain relationship of reinforcing bars including buckling", Engineering Structures, Elsevier, 1997: Vol. 19, No.10 pp. 822-826.
6. PAULAY T. AND PRIESTLEY M. J. N. "Seismic Design of Reinforced Concrete and Masonry Buildings", John Wiley & Sons, Inc, USA, 1992.
7. WALRAVEN J. Part 3.3.5 of fib Bulletin 1. Structural Concrete, Textbook on Behaviour, Design and Performance, vol 1. Updated knowledge of the CEB/FIB Model Code 1990.
8. CEN. PrEN 1998 Part 3- "Eurocode 8: Design of structures for earthquake resistance - Part 3: Strengthening and repair of buildings" - Doc CEN/TC250/SC8/N343. (January 2003)